Solitary versus shock wave acceleration in laser-plasma interactions

Andrea Macchi,* Amritpal Singh Nindrayog, and Francesco Pegoraro
Istituto Nazionale di Ottica, Consiglio Nazionale delle Ricerche, Research Unit "Adriano Gozzini," I-56124 Pisa, Italy and Dipartimento di Fisica "Enrico Fermi," Università di Pisa, Largo B. Pontecorvo 3, I-56127 Pisa, Italy
(Received 28 November 2011; revised manuscript received 14 March 2012; published 2 April 2012)

The excitation of nonlinear electrostatic waves, such as shock and solitons, by ultraintense laser interaction with overdense plasmas and related ion acceleration are investigated by numerical simulations. Stability of solitons and formation of shock waves is strongly dependent on the velocity distribution of ions. Monoenergetic components in ion spectra are produced by "pulsed" reflection from solitary waves. Possible relevance to recent experiments on "shock acceleration" is discussed.

DOI: 10.1103/PhysRevE.85.046402 PACS number(s): 52.38.−r, 41.75.Jv

I. INTRODUCTION

In the interaction of superintense ($I = 10^{18}$–$10^{21}\,\mathrm{W\,cm^{-2}}$) laser pulses with overdense plasmas (i.e., having electron density $n_e > n_c = m_e\omega^2/4\pi e^2$, the cutoff or critical density, with ω the laser frequency), the light pressure ranges from gigabar to gerabar values and, like a piston, may sweep out and compress the laser-produced plasma pushing its surface at nearly relativistic speeds. Such a combination of strong compression and acceleration is often described as the generation of strong shock waves (briefly, shocks) propagating toward the bulk of the plasma. These light-pressure-driven shocks may cause heating of solid targets, as experimentally inferred [1], and be of interest for the production of warm dense matter. In addition, shocks may lead to acceleration of ions if the latter are reflected by the shock front as a moving wall. In moderately overdense and hot plasmas, where the shock waves are of a collisionless nature, shock acceleration may lead to both higher ion energies and narrower ion spectra than the widely studied target normal sheath acceleration (TNSA) mechanism [2], as suggested on the basis of numerical simulations [3,4]. Recently, two experiments employing hydrogen gas jet targets and CO_2 lasers reported on monoenergetic proton beams produced via shock acceleration [5,6]. The study of laser-driven shocks in the laboratory may also help the understanding of similar processes in astrophysical environments (see Ref. [7] and references therein). The above-mentioned simple picture of ion acceleration indicates that, as long as the shock velocity v_s is constant, the reflected ions should have velocity $2v_s$ and produce a monoenergetic peak in the spectrum. Silva *et al.* [3] reported that such a peak would evolve into a spectral plateau due to further acceleration in the sheath field at the rear side of the target, so that suppression of such a field (for instance, by producing a smooth density gradient at the rear side) could preserve monoenergeticity. However, in the present paper we show that obtaining monoenergetic spectra is not straightforward, even when neglecting the side effect of the sheath field. We observe monoenergetic peaks in the simulations only when short-duration ion bunches are accelerated by *solitary* waves generated by the laser-plasma interaction. Moreover, the formation and the evolution of both solitonlike or shocklike waves is highly dependent on the velocity distribution of background ions. A crucial point is that, for a ion distribution without a velocity spread, either *all* the ions or *none* of them may be reflected from a moving electrostatic field front, depending on the ratio $\Phi_{\max}/v_s^2$, where $\Phi_{\max}$ is the potential jump at the front. In the first case, a strong loading of the moving structure occurs, causing deceleration and collapse of the shock or soliton and a consequent broadening of the reflected ions' spectrum.

II. BACKGROUND THEORY AND SIMULATION SET-UP

Before describing our simulation results we briefly recall some key aspects of the fluid theory of collisionless electrostatic shocks and solitons [8]. The most relevant point for what follows is that the existence of reflected ions is *integral* to collisionless shocks and not a secondary effect; it may be used as a signature of true shock formation in the simulations. When reflected ions are absent, solutions corresponding to electrostatic *solitons* are found. Hence a necessary and general condition for such solitons to exist with a velocity v_s is that the electrostatic potential energy jump $e\Phi$ has a peak value

$$e\Phi_{\max} < m_i v_s^2/2, \tag{1}$$

so that background ions are not reflected by the soliton. Within the fluid theory with the electrons in an isothermal Boltzmann equilibrium [8] at the temperature T_e, the condition on the potential poses an upper limit on the Mach number $M = v_s/c_s < 1.6$, where $c_s = \sqrt{T_e/m_i}$ is the speed of sound. The other condition is that the soliton must be supersonic, i.e., $M > 1$.

Since we focus on basic aspects we restrict the discussion to one-dimensional particle-in-cell simulations for the sake of simplicity and high numerical resolution. As found in previous work [3], with respect to the 1D modeling the main differences found in two-dimensional (2D) simulations are that the shock front is obviously non-planar, and that the intensity distribution in the focal spot leads to a radial dependence of the initial shock velocity, since the latter is determined by the local amplitude of the laser pulse (see below), in a way analogous to hole boring acceleration in 2D [9]. The simulations in Ref. [3] showed only a few per cent difference in the energy cut-off of ions between 1D and 2D, with the most energetic ions located along the axis (a feature which is common to other acceleration schemes). For what concerns the later evolution of

*andrea.macchi@ino.it

the shock, with respect to a "realistic" 3D geometry we expect the 1D approximation to be reliable as far as the distance travelled by the shock remains smaller than the laser spot width, that is typically of several laser wavelenghts; since the below described phenomena occur already when the shock has travelled only over a few wavelenghts, we expect our findings not to be limited to the 1D, planar geometry.

On the other hand, the issue of higher numerical resolution (which is accessible in 1D) is very important because we found that the numerical results converged only for sufficiently high values of the number of particles per cell N_p, although qualitatively similar features were observed also for lower N_p. This suggests that kinetic effects play an essential role and thus low-density tails in the distribution functions must be resolved accurately. In addition, recent experiments on monoenergetic shock acceleration have shown narrow monoenergetic peaks that apparently contain a very low number of ions [6]; thus, whatever the mechanism of ion acceleration, a multidimensional simulation with insufficient particle statistics would be not able to resolve such features. In the simulations reported below, $N_p = 800$ and the spatial and temporal resolution $\Delta x = c\Delta t = \lambda/400$, where λ is the laser wavelength. Two-dimensional simulations with such values of N_p and Δx would be extremely demanding on the computational side and are left for future work.

III. SIMULATION RESULTS

A. Solitary acoustic waves

We now analyze a representative simulation with the following setup. The laser pulse was linearly polarized with a peak amplitude $a_0 = 16$, where $a_0 = 0.85(I\lambda^2/10^{18}\ \mathrm{W\,cm^{-2}}\,\mu\mathrm{m}^2)^{1/2}$, and duration $\tau = 4T$ [full width at half maximum (FWHM)], with T the laser period; the temporal profile was composed of $1T$ long, $\sin^2$-like rising and falling ramps and a $3T$ plateau. The plasma had a slab, squarelike profile with initial ion and electron densities $n_i = n_e = n_0 = 20n_c$ and 15λ thickness. Ions were protons ($Z = A = 1$). For reference, the laser pulse front reaches the front surface placed at $x = 0$ at time $t = 0$.

Eight snapshots of the profiles of ion density n_i and longitudinal electrostatic field E_x and of the $f_i(x, p_x)$ phase-space distribution of ions are shown in Fig.1. In the early stage of the interaction, the laser pulse accelerates a fraction of strongly relativistic electrons with an energy of several $m_e c^2$, which penetrate the target and later recirculate across it, driving heating of bulk electrons. A solitary structure is generated at the front surface under the action of the laser pulse and then propagates into the plasma bulk at a constant velocity $v_s \simeq 0.05c$. This value is close to the hole boring velocity v_{HB} [9,10], which in our case is given by

$$v_{\mathrm{HB}} = a_0 c \left(\frac{1+R}{2}\frac{Z}{A}\frac{m_e}{m_p}\frac{n_c}{n_e}\right)^{1/2}, \qquad (2)$$

where the reflection coefficient is measured to be $R \simeq 0.75$ in the simulation of Fig. 1, yielding $v_{\mathrm{HB}} \simeq 0.06c$. At $t = 65T$, the solitary structure is located at $x \simeq 3.7\lambda$ (first frame of Fig. 1). The ion density has a very strong spike, reaching values up to $\simeq 9$ times the background density. The electric field around the density spike has a sawtooth shape. For reference we call the structure we observe a solitary acoustic wave (SAW). The snapshots of the SAW density and field profiles are qualitatively similar to those of electrostatic solitons as described in Ref. [8]. However, several of the dynamics features we describe below are not found within standard fluid theory.

Numerical integration of E_x over x for the SAW at $t = 65T$ (first snapshot in Fig. 1) yields $e\Phi_{\max} \simeq 0.78E_0\lambda \simeq 4.9m_e c^2$. Since $m_i v_s^2/2 \simeq 2.3m_e c^2 < e\Phi_{\max}$ one would expect ion reflection to occur promptly from the SAW field. This indeed occurs in the simulation, producing a bunch of high-energy ions with very small momentum spread, as can be observed at $t = 70T$ and $75T$. However, violation of the condition (1) and consequent ion reflection do not destroy the SAW; at $t = 75T$, the SAW is still present with almost unperturbed velocity and ion reflection has stopped. Between $t = 75T$ and $85T$ a second bunch is formed in a very similar way, as observed between the third and fifth snapshots in Fig. 1. Both bunches correspond to a monoenergetic high-energy peak in the spectrum, as shown in Fig. 2(a); the FWHM of the peak at $t = 75T$ is less than 1%.

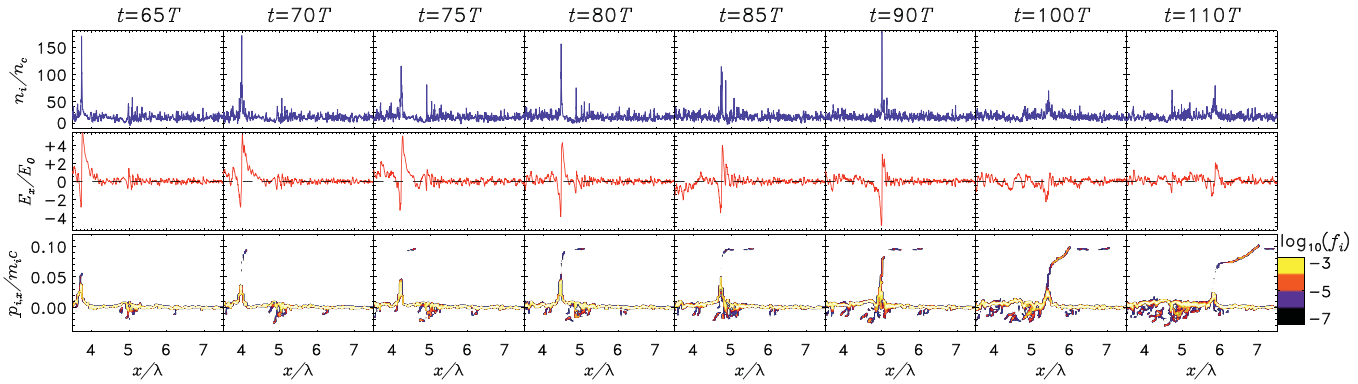

FIG. 1. (Color online) Snapshots of the evolution of a solitary acoustic wave at eight different times. The top, middle, and bottom rows show the ion density n_i, the electrostatic field E_x, and the contours of the $f_i(x, p_x)$ ion phase-space distribution on a $\log_{10}$ scale, respectively. The laser pulse impinges from the left, reaching the plasma boundary ($x = 0\lambda$) at $t = 0T$. Simulation parameters are $a_0 = 16$, $\tau = 4T$, and $n_e = 20n_c$. Furthermore, n_i is normalized to n_c, E_x is normalized to $E_0 = m_e\omega c/e$, and p_x is normalized to $m_p c$.

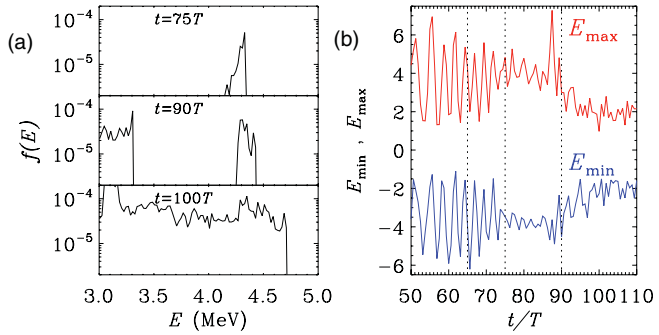

FIG. 2. (Color online) (a) Ion spectra from the simulation of Fig. 1 at the times $t = 75T$, $90T$, and $100T$. Only ions in the same spatial range as in Fig. 1, i.e., $3.5 < x < 7.5$, are included in the spectra. (b) Temporal evolution of the maximum (red line) and the minimum (blue line) values of the electric field for the SAW structure observed in Fig. 1. The vertical dashed lines mark the instants $t = 65T$, $75T$, and $90T$ at which ion-reflection events start, as seen in Fig. 1.

The acceleration of a third bunch at $t = 90T$ is correlated with a much stronger perturbation of the SAW whose amplitude and velocity decrease. As a consequence, the high-energy part of the spectrum broadens and monoenergetic features are lost, as seen in Fig. 2(a) at $t = 100T$.

The apparent behavior of the SAW is related to the observation that the electric-field amplitude is not constant in time, as for the standard soliton solution, but *oscillates* as shown in Fig. 2. The temporal behavior of the maximum and minimum values shows that the electron cloud around the ion density spike oscillates back and forth. The oscillation is quenched after the generation of the second fast bunch at $t \simeq 75T$. At this instant, the potential jump at the SAW front is $e\Phi_{\max} \simeq 0.5E_0\lambda \simeq 3.1m_ec^2$, slightly above the stability threshold (1). Eventually, the overall amplitude greatly decreases after the generation of the third bunch, as also observed in the last frames in Fig. 1. Apparently, such collapse of the SAW occurs after a collision with a slower, counterpropagating structure, which can also be noticed in the frames of Fig. 1.

B. Effects of the ion velocity distribution

The above-reported observations led us to infer that the local velocity distribution of ions has a crucial role in determining both the stability of solitary waves and the possibility to generate true shocks whose signature would be, in the framework of fluid theory, the formation of a continuous flow of reflected ions. If the ions are cold, i.e., have no energy spread, reflection from a moving potential barrier may occur for either none or all of the ions. In the latter case, the wave would quickly lose its energy in the attempt to accelerate the whole bulk of ions.

In order for a collisionless shock to form, it must be possible for the wave to pick up from the ion distribution only a fraction of the ions in an energy range for which a reflection condition analogous to Eq. (1) is fulfilled. If the ion distribution has a velocity spread, for a given value of $\Phi_{\max}$ all ions with velocity $v_r > v_s - \sqrt{2e\Phi_{\max}/m_i}$ will be reflected from the front. Thus a true shock may form in the presence of a sufficiently warm ion distribution. Figure 3 shows results of a simulation with identical parameters as Fig. 1, but with the initial ion temperature $T_i = 5$ keV. Formation of a shocklike structure with steady reflection of ions is observed. The shock front velocity is found to decrease in time, which may be interpreted as due to the wave energy transfer into reflected ions. As a consequence, with respect

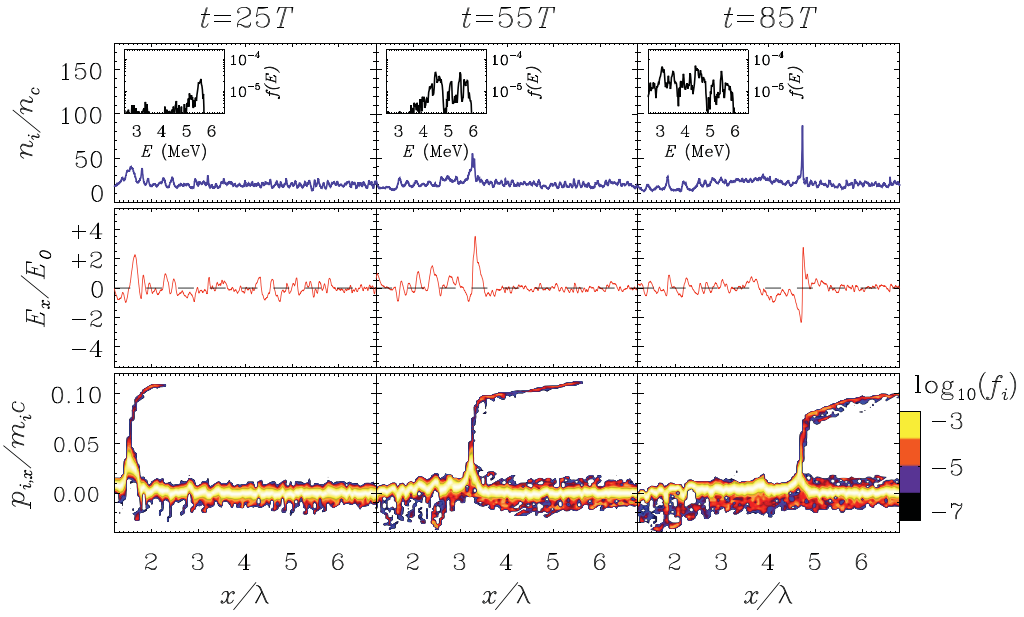

FIG. 3. (Color online) Snapshots at three different times of the n_i, E_x, and $f_i(x, p_x)$ for a simulation identical to that of Fig. 1 but for an initial ion temperature $T_i \simeq 10^{-2}m_ec^2 = 5$ keV, showing the onset of steady ion reflection. The scales are the same as in Fig. 1 to show that the perturbation in n_i and E_x has a lower value in the present case. The insets show the corresponding ion spectra, limited to the ions in the region around the shock and excluding ions accelerated at the target boundaries.

to the cold-ion case, narrow monoenergetic peaks almost never appear at any time in the spectrum (see the insets in Fig. 3) and the high-energy tail progressively broadens toward lower energies, although the cutoff energy is a bit higher with respect to the cold case. Thus, in this case, a spectral plateau is produced because of shock deceleration rather than due to further acceleration of the reflected ions in the rear side sheath. Some modulations are apparent in both the phase-space density and the spectral plateau of reflected ions; they may be related to the oscillation of the electric field at the wave front, similar to Fig. 2.

The effect of the background ion distribution can be evidenced also by studying a case with parameters identical to Fig. 1 but with a shorter length of the plasma 3λ. In this case, not shown here for brevity, the SAW generated at the front side of the plasma eventually reaches the rear side and propagates in the expanding sheath until it reaches the region in which the ion velocity is such that the ions are now reflected by the SAW potential (since the ions in the sheath move in the same direction of the SAW, their velocity in the rest frame of the SAW is lower than in the laboratory frame, hence they are reflected more easily). From this point on the SAW quickly loses its energy in accelerating ions and collapses. A similar mechanism was also described by He *et al.* [4] and Zhidkov *et al.* [11].

C. Long pulses: multipeak structures

When the laser pulse duration is increased with respect to the above-reported simulations, we observe multiple peaks of the ion density and sawtooth spatial oscillations of the electric field. Although a structure showing multiple oscillations behind a front is reminiscent of a collisionless shock wave as seen in textbooks, again we generally do not observe a steady ion reflection at the front. The density peaks move at different velocities and thus disperse in time. Hence the structure may be interpreted as a multipeak SAW, generated due to pulsed hole boring acceleration [9] at a rate that is approximately the same for simulations having the same pulse intensity and plasma density, so that a longer pulse duration allows acceleration of a sequence of ion bunches.

A representative long pulse simulation is shown in Fig. 4. The laser pulse has peak amplitude $a_0 = 16$ (like the above-reported short pulse simulations) with $5T$ rise and fall ramps and a $60T$ plateau. The plasma density and thickness are $10n_c$ and 15λ, respectively. These parameters are close to those of previously reported one-dimensional simulations (see Fig. 1 in Ref. [3]) and indeed some features observed in the ion phase space and density profiles look very similar. However, in our simulations the higher number of computational particles allows us to highlight additional details in the phase-space distribution of Fig. 4 (bottom row) such as vortex structures behind the front, corresponding to trapped ions bouncing between adjacent peaks, where a potential well is formed. The observation of ions trapped in the multipeak, nonlinear structure of the electric field and the quite broad distribution along the momentum axis of the most energetic ions suggest that the latter may actually be accelerated by surfing the longitudinal wave structure rather than being merely reflected by the field at the front. In addition, we observe significant oscillations of the electric field *ahead* of the wave front (i.e., of the rightmost density peak in Fig. 4), which may have been excited by fast electrons and are related to modulations in the momenta of the highest-energy ions. The spectrum of the latter is quite broad (inset of Fig. 4) even when neglecting the contribution of TNSA at the rear side.

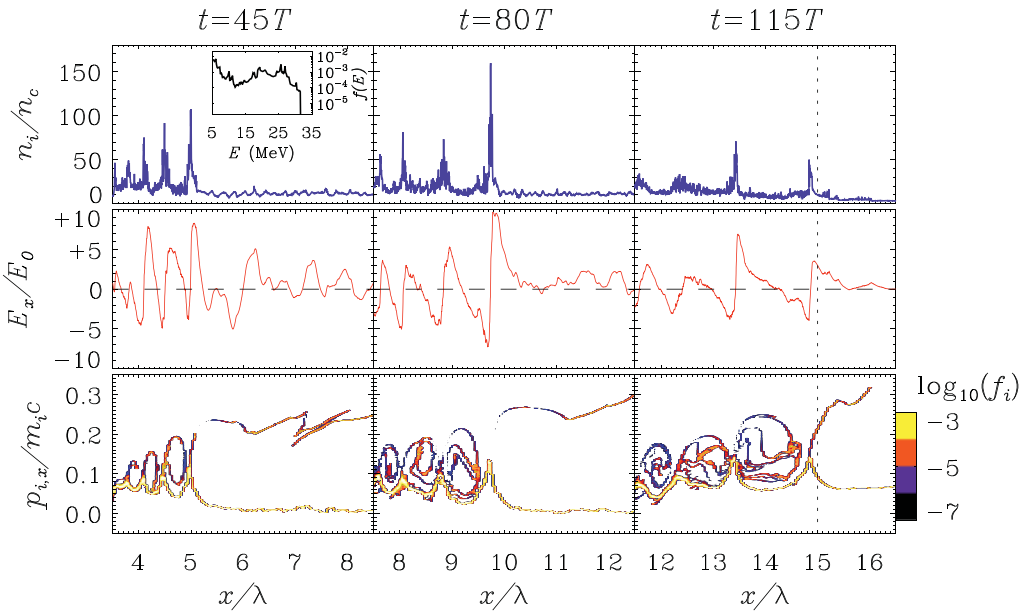

FIG. 4. (Color online) Snapshots of multipeak structures at three different times from a long pulse simulation. The inset shows the spectrum at $t = 45T$, limited to the ions in the same region as the plots. The vertical dashed line marks the initial position of the rear side of the target. Simulation parameters are $a_0 = 16$, $\tau = 65T$, and $n_e = 10n_c$. Units are the same as in Fig. 1.

IV. DISCUSSION AND COMPARISON WITH EXPERIMENTS

Our study suggests that generating highly monoenergetic ions by shock acceleration is not straightforward, as in our simulation we observe narrow spectra only as resulting from SAW pulsations and as a transient effect, since, as shown in Figs. 1 and 2, the SAW collapse ultimately produces a broad spectrum masking the monoenergetic peak. Producing a monoenergetic spectrum might not coexist with efficiency because the reflection of a large fraction of ions by the moving structure (either a shock or a soliton) would ultimately cause a strong loading effect decreasing its field and velocity. This is in qualitative agreement with the experimental results of Haberberger *et al*. [6], where the number of ions ($\sim 2.5 \times 10^5$) in the narrow spectral peak at $\sim$22MeV implies a conversion efficiency $< 10^{-8}$ of the 60−J pulse energy. A direct comparison of our simulations with the experiment in Ref. [6], which involves several additional issues such as the pulse shape and the plasma profile, is beyond the scope of the present paper.

All of the above-described effects related to SAW generation, dynamics, and acceleration of ions in the *bulk* are observed only with linear polarization, for which electrons are heated up to relativistic energies. For circular polarization, no ion acceleration occurs in the bulk. Although Palmer *et al*. [5] report on "protons accelerated by a radiation-pressure-driven shock", we find that the experiment can be better described as evidence of hole boring acceleration [9,10]. Nevertheless, the two different mechanisms might produce similar ion spectra because the velocity of the shock launched at the surface is of the order of v_{HB} [Eq. (2)], while the hole boring process produces via wave breaking ion bunches of velocity $v_i \simeq 2v_{\mathrm{HB}}$ [9] as if the ions were reflected from the plasma surface as a piston driven by light pressure [12].

V. CONCLUSIONS

In conclusion, in our simulations we observe the laser-driven generation of nonlinear, collisionless acoustic waves having either a solitary or a multipeak structure depending on the laser pulse duration. In particular we observe a pulsation of solitary waves leading to the generation of small numbers of monoenergetic ions. In a cold-ion background, wave loading effects prevent true shock wave formation and efficient monoenergetic acceleration. In general, the dynamics of shock acceleration in the plasma bulk appears to be more complex than the simple picture of reflection from a moving wall.

ACKNOWLEDGMENTS

This work was supported by the Italian Ministry for University and Research through the FIRB Futuro in Ricerca project "Superintense Laser-Driven Ion Sources".

[1] K. U. Akli *et al*., Phys. Rev. Lett. **100**, 165002 (2008).
[2] S. C. Wilks, A. B. Langdon, T. E. Cowan, M. Roth, M. Singh, S. Hatchett, M. H. Key, D. Pennington, A. MacKinnon, and R. A. Snavely, Phys. Plasmas **8**, 542 (2001).
[3] L. O. Silva, M. Marti, J. R. Davies, R. A. Fonseca, C. Ren, F. Tsung, and W. B. Mori, Phys. Rev. Lett. **92**, 015002 (2004).
[4] M. Q. He, Q.-L. Dong, Z.-M. Sheng, S.-M. Weng, M. Chen, H.-C. Wu, and J. Zhang, Phys. Rev. E **76**, 035402 (2007).
[5] C. A. J. Palmer, N. P. Dover, I. Pogorelsky, M. Babzien, G. I. Dudnikova, M. Ispiriyan, M. N. Polyanskiy, J. Schreiber, P. Shkolnikov, V. Yakimenko, and Z. Najmudin, Phys. Rev. Lett. **106**, 014801 (2011).
[6] D. Haberberger, S. Tochitsky, F. Fiuza, C. Gong, R. A. Fonseca, L. O. Silva, W. B. Mori, and C. Joshi, Nature Phys. **8**, 95 (2012).
[7] S. F. Martins, R. A. Fonseca, L. O. Silva, and W. B. Mori, Astrophys. J. Lett. **695**, L189 (2009) .
[8] D. A. Tidman and N. A. Krall, *Shock Waves in Collisionless Plasmas* (Wiley-Interscience, New York, 1971), Chap. 6.
[9] A. Macchi, F. Cattani, T. V. Liseykina, and F. Cornolti, Phys. Rev. Lett. **94**, 165003 (2005).
[10] A. P. L. Robinson, P. Gibbon, M. Zepf, S. Kar, R. G. Evans, and C. Bellei, Plasma Phys. Controlled Fusion **51**, 024004 (2009).
[11] A. Zhidkov, M. Uesaka, A. Sasaki, and H. Daido, Phys. Rev. Lett. **89**, 215002 (2002).
[12] For the sake of clarity we further notice that both the interaction regime and the nature of solitary waves investigated in the present paper are fundamentally different from the ones studied by D. Jung *et al*., Phys. Rev. Lett. **107**, 115002 (2011), where mononergetic ion acceleration is related to the generation of electromagnetic "ion solitary waves" by the interaction of circularly polarized pulses with ultrathin targets.